EBioMedicine 41 (2019) 610–622

Contents lists available at ScienceDirect

EBioMedicine

journal homepage: www.ebiomedicine.com

EBioMedicine
Published by THE LANCET

Anti α-enolase antibody is a novel autoimmune biomarker for unexplained recurrent miscarriages

Yao Ye [a], Christina Kuhn [a], Miwako Kösters [b], Georg J. Arnold [b], Hellen Ishikawa-Ankerhold [c], Christian Schulz [c], Nina Rogenhofer [a], Christian J. Thaler [a], Sven Mahner [a], Thomas Fröhlich [b], Udo Jeschke [a,*,1], Viktoria von Schönfeldt [a,1]

[a] Department of Obstetrics and Gynaecology, University Hospital, Ludwig-Maximilians-University, 81377 Munich, Germany
[b] Laboratory for Functional Genome Analysis LAFUGA, Gene Center, Ludwig-Maximilians -University, 81377 Munich, Germany
[c] Medizinische Klinik und Poliklinik I, Klinikum der Universität München, Ludwig-Maximilians -University, 81377 Munich, Germany

ARTICLE INFO

Article history:
Received 20 November 2018
Received in revised form 7 February 2019
Accepted 13 February 2019
Available online 1 March 2019

Keywords:
Unexplained recurrent miscarriages
Anti-trophoblast antibodies
JEG-3 cells
Anti-α-enolase antibodies

ABSTRACT

Background: We recently demonstrated the increased abundance of anti-trophoblast antibodies (ATAB) in sera of patients with unexplained recurrent miscarriages (uRM). Further, the ATAB-positive sera bound to JEG-3 human choriocarcinoma cells in vitro, resulting in decreased productions of β-human chorionic gonadotropin (β-hCG) and progesterone in these cells. However, the specific antigenic epitopes of ATAB have remained unknown. Therefore, it was the aim of this study to determine specific targets of ATAB in uRM patients.

Methods: Potential targets of ATAB were analyzed by 2-dimensional difference gel electrophoresis (2D-DIGE) and mass spectrometry, and thereby identifying α-Enolase (ENO1). ATAB targeting of ENO1 was further confirmed in a competitive binding assay. Levels of anti-ENO1 antibodies as well as β-hCG and progesterone were quantified with enzyme-linked immunosorbent assay (ELISA). Additionally, expression of ENO1 was analyzed in first trimester placentas by immunohistochemistry and immunofluorescence analysis.

Findings: We here identified ENO1 as a prominent target of ATAB. Serum levels of anti-ENO1 antibodies were increased in ATAB-positive compared to ATAB-negative patients. Further, increased expression of ENO1 and its co-expression with β-arrestin was found in the extra villous trophoblasts of uRM patients in first trimester placentas. In vitro, anti-ENO1 antibodies decreased the secretion of β-hCG and progesterone in JEG-3 and primary human villous trophoblast cells.

Interpretation: Serum anti-ENO1 antibodies might be an autoimmune biomarker for uRM. Targeting the formation of anti-ENO1 antibodies or inhibition of ENO1 expression could potentially represent therapeutic strategies for these patients.

Fund: All authors declare no conflict of interest. Yao Ye was supported by the China Scholarship Council. Hellen Ishikawa-Ankerhold and Christian Schulz were supported by the SFB914, projects Z01 and A10. None of the rest authors has any conflict of interest to declare.

1. Introduction

Recurrent miscarriages (RM) are defined as two or more pregnancies that have failed consecutively before the 20th week of pregnancy according to the Practice Committee of the American Society for Reproductive Medicine [1]. RM affects 1% of women worldwide [2]. Causes of RM include cytogenetic abnormalities, anatomic factors, inherited thrombophilia, infection, hormonal and metabolic factors, antiphospholipid syndrome, male factors, alloimmune factors, psychological factors, as well as lifestyle and environmental factors [3]. 50% of RM patients are classified as unexplained RM (uRM) patients, remaining without a specific etiology after thorough and systematic work up of possible etiologic factors [2]. The prognosis for a live birth in uRM women is 50% to 80% without supportive care or interventions [4].

It is believed that uRM is associated with the aberrant expression of immunological factors during pregnancy. So far studies have focused on immunological factors in uRM, such as human leukocyte antigens (HLA), anti-trophoblast antibodies (ATAB), anti-endometrial antibodies, antisperm antibodies, cytokines, the leukaemia inhibitory factor (LIF), T-cells, peripheral natural killer cells [3,5]. HLA-G is the major

* Corresponding author at: Ludwig-Maximilians University of Munich, Department of Obstetrics and Gynecology, Campus Großhadern: Marchioninistraße 15, 81377 Munich, Germany.
E-mail address: Udo.Jeschke@med.uni-muenchen.de (U. Jeschke).
[1] Contributed equally as senior authors.

https://doi.org/10.1016/j.ebiom.2019.02.027

Research in context section

Evidence before this study

We previously demonstrated that anti-trophoblast antibodies (ATAB) are more prevalent in uRM patients than healthy controls. The identification and quantification of ATAB is restricted to JEG-3 cell model. ATAB-positive sera inhibit the production of β-hCG and progesterone in JEG-3 human choriocarcinoma cells. The specific antigens of ATAB and the corresponding antibodies in uRM were unknown.

Added value of this study

We identified ENO1 as a prominent target of ATAB. Anti-ENO1 antibodies decreased the secretion of β-hCG and progesterone in JEG-3 and primary human villous trophoblast cells. Compared to ATAB-negative cases, serum levels of anti-ENO1 antibodies were elevated in ATAB-positive uRM patients. Overexpression of ENO1 in extra villous trophoblasts and the co-expression of ENO1 and β-arrestin might lead to anti-ENO1 autoimmune antibodies in uRM patients.

Implications of all the available evidence

uRM might be an autoimmune disease with high levels of anti-ENO1 antibodies in blood serum. The identification of ENO1 as a target for ATAB production enables us to search for a possible treatment of uRM in the future.

histocompatibility complex expressed in extra villous trophoblasts (EVT) which may affect fetal development and survival. The expression of HLA-G in EVT promotes trophoblast invasiveness, decidual cell differentiation, vascular remodeling and immunosuppression [6]. Patients carrying the HLA-G 3'UTR haplotype showed a reduced risk of RM [7]. Serum HLA and HLA-C antibody levels were higher in RM women compared to healthy controls [8].

The occurrence of uRM might also be related to antibodies cross-reacting with the HLA-negative syncytiotrophoblast [9]. ATAB are defined as maternal immunoglobulins directed against fetal trophoblast antigens and therefore influencing blastocyst formation, implantation and pregnancy [5]. ATAB exist in both healthy pregnant women and RM patients [10]. The precise identity of ATAB as well as the non-HLA specific antigenic epitopes targeted by ATAB remained unknown. Kajino et al. used chorionic villous plasma membranes as trophoblast antigens to detect ATAB [10]. Hanna et al. applied indirect immunofluorescence with placenta cells serving as targets to examine ATAB in the sera of uRM women [11]. Trophoblasts contain many immunologically allotypic proteins and maternal antibodies against these proteins which are thought to play a role in reproductive failure [5]. Therefore, it is of vital importance to detect the ATAB contributing to miscarriages and to exactly identify their specific target antigens in the trophoblast.

JEG-3 choriocarcinoma cells express MHC class I antigen HLA-G but are HLA-A and HLA-B negative [12,13]. With JEG-3 cells serving as the trophoblast target, our group previously demonstrated that ATAB are more prevalent in the sera of uRM patients in comparison to healthy controls, and that the reactivity of ATAB is increased in patients with higher frequency of miscarriages [12]. In order to further explore the effect of ATAB, we divided all uRM patients into ATAB-positive patients and ATAB-negative patients. We found that compared with sera of healthy controls, sera of ATAB-positive women inhibited the secretion of β-hCG and progesterone in JEG-3 cells, while the sera of ATAB-negative patients did not alter JEG-3 function [14].

In the current study, we aimed to identify possible targets of ATAB and its effects on JEG-3 and human villous trophoblast (HVT) cells. Therefore, we isolated and purified IgGs from sera of uRM patients. Mass spectrometry revealed ENO1 as a novel target of ATAB which could be of potential relevance in uRM.

2. Materials and methods

2.1. Study design

ATAB has been previously described on JEG-3 cells, and the identification and quantification of ATAB are restricted to this cell model [12,14,15]. It is a retrospective study designed to assess the ATAB reactivity among uRM patients in order to explore the possible targets of ATAB. We designed a case control study from the original trial population and divided them into ATAB-positive group and ATAB-negative group according to the ATAB reactivity. Furthermore, ATAB-positive IgGs and ATAB-negative-IgGs were obtained by isolation and purification of IgGs from the sera of both groups. Afterwards, we investigated the possible antigens of ATAB and the effect of ATAB-positive IgGs on the function of JEG-3 cells. The JEG-3 membrane lysate served as antigens and the purified ATAB-positive IgGs as antibodies. With western blots and mass spectrometry, we found α-Enolase (ENO1) to be one of the possible targets of ATAB. Then we evaluated the effect of anti-ENO1 antibodies on JEG-3 cells and human villous trophoblast (HVT) cells, the level of anti-ENO1 antibodies in the sera of uRM patients as well as the expression of ENO1 in the first trimester uRM placenta (Fig. 1).

2.2. Trophoblast models

Choriocarcinoma cell line JEG-3 (ATCC HTB-36, Manassas, USA) served as the tool for the identification of ATAB in our study. JEG-3 cells resemble EVT that are exposed to maternal decidua and blood. Human villous trophoblast (HVT) cells are isolated from human placental villi (ScienCell, USA) and served as the human primary trophoblast cells. Both, JEG-3 cells and HVT cells were cultured in RPMI 1640 medium + Gluta MAX™ (Gibco, USA) supplemented by 10% fetal bovine serum (FCS, Gibco, USA).

2.3. Ethical approval

The study was approved by the ethical committee of the Medical Faculty, Ludwig-Maximilian-University of Munich (Approval Number: 337–06) and informed consent was obtained from each patient in written form. Patients' blood samples, placental specimens and clinical information were anonymized and encoded for statistical workup.

2.4. Patient blood samples

Patients with a history of at least two uRM before 20th weeks of gestation were pooled and consented in this study between July 2014 and December 2017. Exclusion criteria for the uRM group have been described thoroughly in our previous studies as well as in Supplementary Table 1 [12,14,15]. All uRM patients were divided into two groups according to the anti-JEG-3 reactivity: ATAB-positive group ($n = 30$) and ATAB-negative group ($n = 36$). The ATAB-positive group was defined as uRM patients with over 39% anti-JEG-3 reactivity, meaning that the anti-JEG-3 reactivity was above 95% confidence interval of controls. The clinical characteristics of these two group patients are summarized in Supplementary Table 2. The sera of uRM patients were used for immunoglobulin Gs (IgGs) isolation and purification, as well as autoimmune antibodies detection.

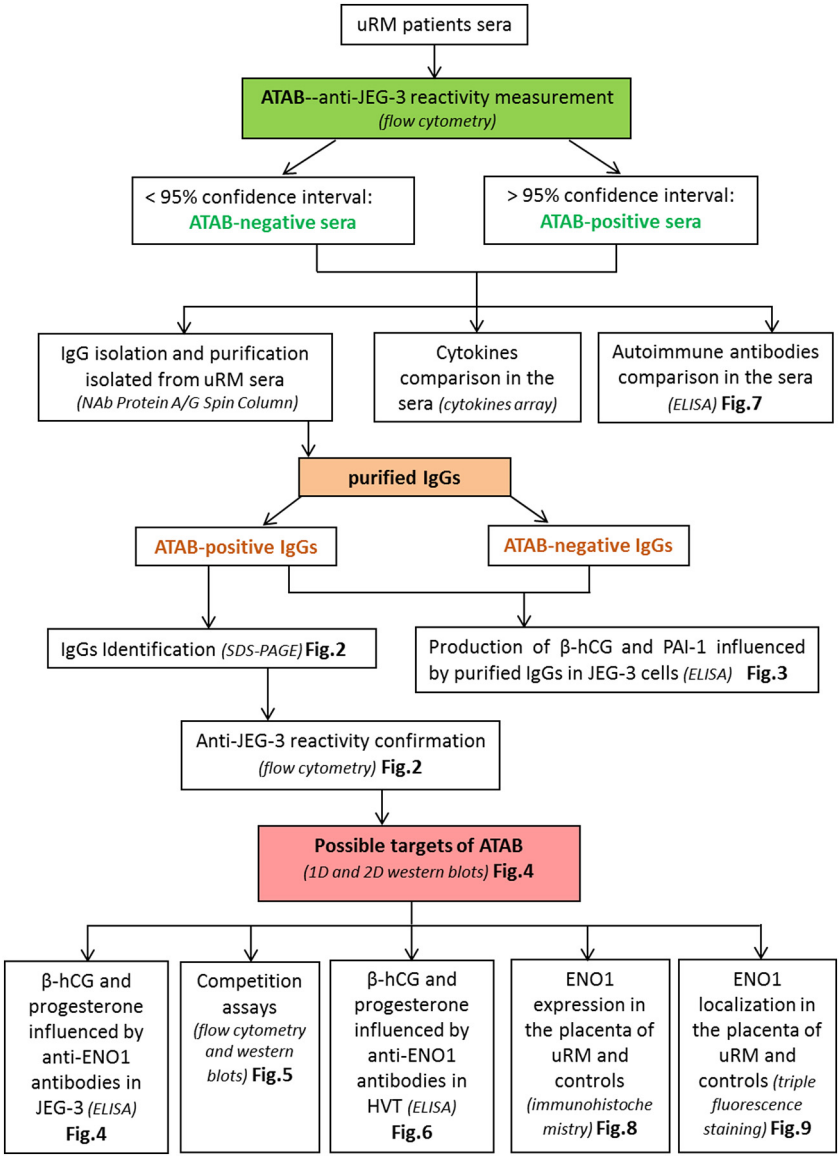

Fig. 1. ATAB study flow charts.

2.5. Placental tissue samples

We analyzed ENO1 expression in placenta tissues of 20 uRM patients and 22 healthy controls, whose clinical characteristics were described in our latest publication [16] and summarized in supplementary Table 3. The controls were with legal pregnancy termination from a private practice in Munich, Germany. Placenta samples were obtained by dilatation and evacuation without any prior pharmaceutical induction. These samples were fixed immediately in 4% buffered formalin for 20–24 h and embedded in paraffin for further immunohistochemical and triple immunofluorescence analysis.

2.6. IgG isolation and purification

Purified IgGs were isolated from the sera of 7 ATAB-positive patients and 7 ATAB-negative patients with the NAb spin column (Thermo Scientific, Waltham, Massachusetts, USA). The serum of each patient was diluted to 2 ml with the binding buffer (0·1 M phosphate, 0·15 M sodium chloride; pH 7·2) and then incubated in the NAb spin column at room temperature for 10 min. Unspecific non-binding proteins were washed away with the binding buffer for three times. Afterwards purified IgGs were detached from the immobilized protein resin with the elution buffer (0·1 M glycine, pH 2·5) and stored in the neutralization buffer (1 M Tris, pH 8·5). Between each step the column was centrifuged to 1000 ×*g* for 1 min. The purified IgGs were transferred into a concentrator column (Thermo Scientific, Waltham, Massachusetts, USA) and centrifuged at the speed of 2500 ×*g* for 45 min. The upper portions of each chamber containing the intense IgGs fractions were dissolved in approximately 100 μl of 4-(2-hydroxyethyl)-1-piperazineethanesulfonic acid (HEPES) and pooled into two tubes according to ATAB reactivity. The concentration of purified IgGs was measured by the Bradford assay (BIO-RAD, Hercules, California, USA) and the optical density (OD) was examined at 595 nm using Elx800 universal Microplate Reader. Lastly, half of the pooled purified IgGs were stored in a 4 °C refrigerator as ready-to-use samples, and the rest was stored as aliquot at −20 °C.

2.7. Flow cytometry

ATAB reactivity was studied as described previously with minor modifications and measured in mean channel shifts (MCS) by flow cytometry [12,15]. To investigate if purified IgGs bind to JEG-3 cells, 2·5 × 10^5 JEG-3 cells were incubated with 20 μg purified IgGs serving as

primary antibodies at 4 °C for 60 min. After washing two times in RPMI buffer, cell suspensions were treated with 1:10 diluted FITC-conjugated goat anti-human secondary antibodies (Dako, Glostrup, Denmark) at 4 °C for 60 min in the darkness. Subsequently, unbound antibodies were washed off and cell suspensions were analyzed on a Becton-Dickinson flow cytometer equipped with a 2.4 mW argon ion laser at an excitation wavelength of 488 nm (FACScan, Heidelberg, Germany). Sera from a patient identified as highly reactive in primary experiments were used as a positive control, while sera of a blood group AB standard samples as the negative control [12].

We performed competition assays in two manners to confirm the ability of anti-ENO1 antibodies to bind to JEG-3 cells by flow cytometry. In the first manner, we first mixed 20 μl rabbit anti-ENO1 antibodies (0·42 mg/ml, Fitzgerald, Acton, Massachusetts, USA) with 20 μg ATAB-positive IgGs. $2·5 \times 10^5$ JEG-3 cells were incubated with the mixed antibodies or 20 μg ATAB-positive IgGs at 4 °C for 60 min, respectively. After washing steps, FITC-conjugated goat anti-human secondary antibodies (Dako, Glostrup, Denmark) were incubated at 4 °C for 60 min in the darkness. The following detection steps were the same as above. For the second manner, we tested if ATAB-positive IgGs could bind to recombinant ENO1 proteins. We pre-incubated 20 μg recombinant human ENO1 proteins (MyBioSource, Southern California, San Diego, USA) and 20 μg BSA with 20 μg ATAB-positive IgGs separately at room temperature for 60 min. Then $2·5 \times 10^5$ JEG-3 cells were added in each tube and incubated at 4 °C for 60 min. After washing, FITC-conjugated goat anti-human secondary antibodies were incubated and followed by the detection as described above.

2.8. Trophoblast cells stimulation

50,000 JEG-3 cells per well were seeded into 24-well plates and incubated with different concentrations of purified IgGs or anti-ENO1 antibodies. 5, 10 and 50 μg/ml of isolated IgGs with positive- or negative-ATAB were added into RPMI1640 with 10% FBS and incubated for 12, 24 and 36 h in a 37 °C 5% CO_2 incubator, respectively. 1, 10, 100 and 1000 ng/ml of polyclonal rabbit anti-ENO1 antibodies (Novus Biologicals, Littleton, Colorado, USA) were incubated with JEG-3 cells for 36 h after removal of sodium azide with NAb spin column. 1 μg/ml polyclonal rabbit IgGs (R&D systems, Minneapolis, Minnesota, USA) served as a normal rabbit IgG control. The supernatants of JEG-3 were collected to quantify β-hCG, progesterone and plasminogen activator inhibitor type 1 (PAI-1) production at responding time points.

To further confirm the effect of anti-ENO1 antibodies on trophoblast cells, HVT cells were incubated with 1, 10 and 100 ng/ml of anti-ENO1 antibodies for 36 h after removal of sodium azide. The production of β-hCG and progesterone in HVT cells were examinated afterwards.

2.9. Hormone measurement

Supernatants of JEG-3 cells in 24-well plates were centrifuged at 13,200 x g for 10 min to remove debris. β-hCG and progesterone quantifications were carried out according to the manufacturer's instructions on an ADVIA Centaur XP auto analyzer (Siemens Medical Solution Diagnostics) as described in our previous publications [17].

2.10. Human cytokine array

Human Cytokine Array Panel A (R&D Systems, Minneapolis, USA) was used to semi-quantify the cytokines in sera of 18 ATAB-positive patients, 19 ATAB-negative patients and 7 healthy controls. The levels of 36 different cytokines, chemokines, and acute phase proteins were tested in a pooled single sample, including complement component 5/ C5a (C5/C5a), CD40 ligand, granulocyte-colony stimulating factor (G-CSF), granulocyte-macrophage colony-stimulating factor (GM-CSF), CXCL1, CCL1, CD54, interferon-γ (IFN-γ), interleukin (IL)-1α, IL-1β, IL-1γα, IL-2, IL-4, IL-5, IL-6, IL-8, IL-10, IL-12p70, IL-13, IL-16, IL-17, IL-17E, IL-23, IL-27, IL-32α, IP-10, C-X-C motif chemokine (CXCL) 10, CXCL11, Chemokine (C-C motif) ligand (CCL)2, Macrophage migration inhibitory factor (MIF), CCL3, CCL4, PAI-1, CCL-5, CXCL12, tumor necrosis factor-α (TNF-α) and soluble triggering receptor expressed on myeloid cells 1 (sTREM-1). For the analysis, the sera of three different groups were pooled to three separate samples and handled as described in the protocol. The average pixel density was analyzed in duplicate spots of each cytokine and compared between the three groups.

2.11. ELISA

The concentrations of PAI-1 in supernatants of JEG-3 cells were measured by Quantikine ELISA Human Serpin E1/PAI-1 Immunoassay (R&D Systems, Minneapolis, USA) after 8 fold concentration with a centrifugal vacuum concentrator (Concentrator 5301, Eppendorf, Germany). Firstly all standards and supernatants were incubated with the microplate coated with a monoclonal antibody specific for PAI-1 for 2 h. After three washes, human Serpin E1/PAI-1 conjugate was incubated for another 2 h. Substrates were incubated in the dark for 30 min, stopped by the stop solution and analyzed in a microplate reader (DYNEX Technologies, MRX II) using wavelengths between 450 and 570 nm. The standards concentrations were 0, 0·313, 0·625, 1·25, 2·5, 5·0, 10·0 and 20·0 ng/ml.

The levels of α-Enolase antibodies, γ-Enolase antibodies, anti citrullinated fibrinogen (anti-CFG) antibodies and anti-modified citrullinated vimentin (anti-MCV) antibodies in the sera of 30 ATAB-positive patients and 36 ATAB-negative patients were detected by quantitative sandwich ELISAs (MyBiosource, Southern California, San Diego, USA) according to the corresponding protocols. The used standards concentrations for anti-ENO1 antibodies were 0·625, 1·25, 2·5, 5, 10, 20 ng/ml, for anti-γ-Enolase antibodies 0·25, 0·5, 1, 2, 4, 8 ng/ml, for anti-CFG antibodies 3·12, 6·25, 12·5, 25, 50, 100 ng/ml and for anti-MCV antibodies 50, 100, 250, 500, 1000 U/ml.

2.12. SDS-PAGE analysis

To characterize purified IgGs from uRM patients' sera, sodium dodecyl sulfate–polyacrylamide gel electrophoresis (SDS-PAGE) was performed in a mini-Gel device (BIO-RAD, Hercules, California, USA) according to the standard procedure and stained with Coomassie blue. For the molecular weight marker, we used the pre-stained markers (SpectraTM Multicolor Broad Range Protein Ladder, Thermo Scientific, USA).

2.13. 1D western blotting

We performed one dimensional western immunoblotting to detect ATAB binders. JEG-3 cells were lysed with radioimmunoprecipatation assay buffer (RIPA, Sigma-Aldrich, St. Louis, Missouri, USA) and mixed with 4× sample buffer (10 mM Tris, 1 mM EDTA, 10% glycerin, 2% SDS, 1% β-mercaptoethanol). 20 μg of JEG-3 cell lysates were separated in 10% SDS-PAGE and electro transferred to a polyvinylidene fluoride membrane (PVDF, Bio-Rad, USA). The membrane was blocked with 4% skim milk powder in 0.02%NaN_3/PBS for 2 h and then incubated with 10 μg/ml positive ATAB IgGs for 16 h at room temperature. After washing, the PVDF membrane was incubated with the goat anti-human secondary antibody conjugated with alkaline phosphatase (1:1000 dilution, Jackson Immuno Research), and detected with 5-bromo-4-chloro-3′-indolylphosphate/nitro-blue tetrazolium (BCIP/NBT)-chromogen substrate solution (Promega). On the basis of 1D western blotting, a competition assay was performed with similar procedures except for the primary antibodies, where a mixture of ATAB-positive IgGs and polyclonal rabbit anti-ENO1 antibodies (Novus Biologicals, Littleton, Colorado, USA) both at a concentration of 10 μg/ml was used.

2.14. 2D western blotting

For two-dimensional gel electrophoresis, JEG-3 cells were lysed with DIGE lysis buffer (7 M urea, 2 M Thio-urea, 30 mM Tris, 4% w/v CHAPS, pH 8·5). The protein concentration of JEG-3 lysates was measured with the Bradford method (BIO-RAD, Hercules, California, USA). Prior to electrophoresis, dried isoelectric focusing (IEF) strips (DryStrips, pH 3–10, 18 cm, GE Healthcare Europe GmbH) were stored overnight in rehydration buffer (8 M Urea, 4% w/v CHAPS, 13 mM DTE, 1% Pharmalyte (pH 3–10)). IEF was done under mineral oil (PlusOne Dry Strip Cover Fluid, GE Healthcare Europe GmbH) using a Multiphor II device (GE Healthcare Europe GmbH) and cup loading at a current of 20 μA per strip for 20 h. Proteins were further focused at 3000 V for 8 h and at 5000 V for 1 h. Before second dimension electrophoresis, IEF strips were incubated for 15 min in equilibration buffer (50 mM Tris-HCl pH 6·8, 6 M urea, 30% v/v glycerin, 2% w/v SDS) containing 1% w/v DTE, followed by a second 15 min incubation step in the same buffer but with 2·5% w/v iodoacetamide instead of DTE. For second dimension SDS gel electrophoresis a ProteanTM II xi device (Bio-Rad, Hercules, USA) and a gel consisting of a 1·5 cm 4% stacking gel (0·5 M Tris-HCl pH 6·8, 4% acrylamide/bis-acrylamide (37·5/1), 0·1% w/v SDS, 0·05% w/v APS, 0·1% v/v TEMED) and a 12% separation gel (1·5 M Tris-HCl pH 8·8, 12% acrylamide/bisacrylamide (37·5/1), 0·1% w/v SDS, 0·05% w/v APS, 0·05% v/v TEMED) was used. IEF gel strips were loaded on the SDS-gel and covered with warm SDS running buffer (25 mM Tris, 192 mM glycin, 0.1% w/v SDS) containing 0·5% w/v agarose. Electrophoresis was done at a constant current of 30 mA/gel for 30 min and at 40 mA/gel for 3 h at 9 °C. In the case were 2D spots had to be visualized, gels were Coomassie stained overnight using 50% v/v methanol, 0.05% w/v Coomassie brilliant blue R-250, 10% v/v acetic acid. Proteins were transferred for 45 min onto a nitrocellulose membrane (pore size: 0.45 μm; Whatman Protran, Dassel, Germany) at 0·8 mA/cm^2. The transfer buffer consisted of 48 mM Tris, 38·6 mM glycin, 0·13% w/v SDS and 20% methanol. To check the transfer efficiency, the membrane was stained using Ponceau S (0·2% w/v Ponceau S, 3% trichloroacetic acid, 3% sulfosalicylic acid in water).

2.15. Mass spectrometry-based identification of proteins

Gel slices were incubated for 15 min in 50 mM NH_4HCO_3. For reduction and alkylation, gel slices were first incubated in 45 mM dithiothreitol / 50 mM NH_4HCO_3 (30 min, 55 °C), followed by an incubation in 100 mM iodoacetamide / 50 mM NH_4HCO_3 (15 min, RT). In case of gel spots, reduction and alkylation was omitted. In-gel digestion was done with 70 ng porcine trypsin (Promega, WI, USA) overnight at 37 °C. The supernatant was recovered and peptides were further extracted from the gel pieces with 80% acetonitrile. The identification of the proteins was either performed on an EASY-nLC 1000 nano-chromatography system (Thermo Scientific, Waltham, MA, USA) online coupled to an Orbitrap XL instrument (Thermo Scientific) or on an Ultimate 3000 chromatography system (Thermo Scientific, Waltham, MA, USA) coupled to a TripleTOF 5600+ mass spectrometer (Sciex, Concord, Canada). Peptide samples were diluted in 0·1% formic acid (FA), transferred to a trap cartridge (PepMap100 C18, 75 μm × 2 cm, 3 μm particles, Thermo Scientific) and separated at a flow rate of 200 nL min^{-1} (column: PepMap RSLC C18, 75 μm × 50 cm, 2 μm particles; Thermo Scientific). In case of 2D spots a 30 min linear gradient from 2% to 50% solvent B (0·1% formic acid, 100% ACN) was used. In case of 1D gel slices, a 120 min long gradient from 2% to 25% followed by a 10 min long gradient from 25% to 50% of solvent B was applied. For MS acquisition, a data-dependent CID method was used. Mass spectrometry data were processed with MASCOT version 2.6.1 (Matrix Science, London, UK) using the human subset of the UniProt database. In case of the 1D gel slice the MASCOT results were filtered for identifications with a probability >95% using Scaffold V4.1 (Proteome Software Inc., Portland, OR, USA).

2.16. Immunohistochemistry

Expression of ENO1 was analyzed in all placenta samples of 20 uRM patients and 22 healthy controls. Paraffin-embedded slides of placentas were dewaxed in xylol and washed in 100% ethanol. All samples were incubated in methanol with 3% H_2O_2 and rehydrated in a descending alcohol series, following by being heated in a pressure cooker using sodium citrate buffer (pH 6·0). After cooling and washing in phosphate-buffered saline (PBS), all slides were incubated with blocking solution (Reagent 1, Zytochem-Plus HRP-Polymer-Kit (mouse/rabbit)) for 20 min to avoid non-specific binding of the primary antibodies. The slides were incubated with anti-ENO1 rabbit IgG polyclonal antibodies (Abcam, ab190365, 1:3000 dilution) at 4 °C for 16 h. After washing, the secondary antibodies/complexes of the ABC detection kits (Vector Laboratories) were applied following the manufacturer's protocols to detect immunostaining reactivity. Immunostaining was visualized with the substrate and the chromogen-3, 3′-diaminobenzidine (DAB; Dako, Glostrup, Denmark) for 30 s. Third-trimester placenta was used as a positive control for the immunohistochemical staining of ENO1 to test antibody function and to determine an appropriate dilution of the antibody for staining. Negative controls were used with the same control tissues and were performed by replacement of a pre-immune serum at the same concentration as the primary antibody (Negative Control for Super Sensitive Rabbit Antibodies, BioGenex, California, USA). All slides were analyzed under the microscope by two independent observers using a Leitz (Wetzlar, Germany) photomicroscope. For the light microscopy analysis, a semi-quantitative IRS score was used [18], which is calculated via the multiplication of optical staining intensity (grades: 0 = no, 1 = weak, 2 = moderate and 3 = strong staining) and the percentage range of positive stained cells (0 = no staining, 1 = ≤10% of the cells; 2 = 11–50% of the cells; 3 = 51–80% of the cells and 4 = ≥81% of the cells were stained for the antibody, respectively).

2.17. Immunofluorescence staining

For the characterization of ENO1 and β-arrestin 2 in the placenta, we used the same paraffin-embedded slides with triple immunofluorescence staining as the slides used for immunohistochemistry. The same experimental steps were carried out as the immunohistochemistry until the step of blocking. Then slides were blocked with a blocking solution (Ultra V Block, Lab Vision, Fremont, CA, USA) for 15 min to avoid non-specific staining and then incubated with ENO1 and β-arrestin 2 primary antibodies overnight at 4 °C. Mouse anti-ENO1 polyclonal IgGs (Abcam, ab190365) were diluted at 1:200 with a diluting medium (Dako, Hamburg, Germany), while rabbit anti-β-arrestin 2 polyclonal IgGs (Abcam, ab151774) were diluted at 1:200. After washing, slides were incubated with Cy2-/Cy3-labeled antibodies (Dianova, Hamburg, Germany) as fluorescent secondary antibodies for 30 min at room temperature in darkness to avoid fluorescence quenching. Cy2-labeled secondary antibodies were used at a dilution of 1:100 and Cy3-labeled antibodies at a dilution of 1:500. Afterwards, slides were incubated with the mouse anti-HLA-G monoclonal IgGs conjugated with biotin (LSBio, Seattle, WA, USA) at room temperature for 1 h. After washing, all slides were incubated with the streptavidin Cy5 conjugated against biotin (Dianova, Hamburg, Germany) for 30 min at room temperature. Confocal laser scanning microscope images were acquired with Zeiss LSM 880 with Airyscan model for high-resolution visualization and analyzed with ZEN blue software. Tissues incubated with the same concentration of secondary antibody served as background controls.

2.18. Statistics

SPSS Statistics 25 was used for data collection, processing and analysis. The Wilcoxon test was used for the evaluation of β-hCG, progesterone, PAI-1, MSC value between two related groups. Mann-Whitney Test

was applied to compare the IRS scores of ENO1 staining in the placenta of uRM patients and healthy controls. Student's *t*-test was used for the comparison of antibody levels in uRM patients and healthy controls. Values with P value <.05 were considered as statistically significant.

2.19. Availability of mass spectrometry data

The mass spectrometry data have been deposited to the ProteomeXchange Consortium via the PRIDE partner repository with the dataset identifier PXD012478 [19].

3. Results

3.1. ATAB-positive IgGs bind to choriocarcinoma cells

The SDS-gel of purified IgGs from uRM patients showed a band pattern typical for IgGs (Fig. 2a). We then carried out flow cytometry to test purified IgGs binding to JEG-3 human choriocarcinoma cells. Reactivity of ATAB with JEG-3 cells was measured in mean channel shifts (MCS). Purified IgGs pooled from ATAB-positive uRM patients bound to JEG-3 cells (MCS value =19·3, Fig. 2b–j).

3.2. Expression of β-hCG and PAI-1 is influenced by purified IgGs

Our previous study proved that sera of ATAB-positive patients inhibit the production of β-hCG and progesterone in JEG-3 cells [14]. In addition, 36 cytokines were analyzed in the sera of 18 ATAB-positive patients, 19 ATAB-negative patients and 7 healthy controls, which include C5/C5a, CD40 ligand, G-CSF, GM-CSF, CXCL1, CCL1, CD54, IFN-γ, IL-1α, IL-1β, IL-1γα, IL-2, IL-4, IL-5, IL-6, IL-8, IL-10, IL-12p70, IL-13, IL-16, IL-17, IL-17E, IL-23, IL-27, IL-32α, IP-10, CXCL 10, CXCL11, CCL2, MIF, CCL3, CCL4, PAI-1, CCL-5, CXCL12, TNF-α and sTREM-1. We identified CD54, CCL2, CCL5 and PAI-1 in serum, among which PAI-1 was the most abundant cytokine and higher expressed in ATAB-positive patients compared to ATAB-negative cases (Supplementary Fig. 1).

To investigate if purified IgGs have the same effects as the sera of uRM patients, JEG-3 cells were incubated with different concentrations of purified IgGs. The production of β-hCG could be reduced from 228·07 ± 20·04 mIU/ml to 192·71 ± 22·25 mIU/ml with 5 μg/ml ATAB-positive IgGs (P = 0·046, Wilcoxon test, Fig. 3a) and to 185·71 ± 25·49 mIU/ml with 10 μg/ml ATAB-positive IgGs (P = 0·018, Wilcoxon test, Fig. 3b) compared with the control after 12 h incubation. In contrast, the secretion of β-hCG was not significantly changed either by

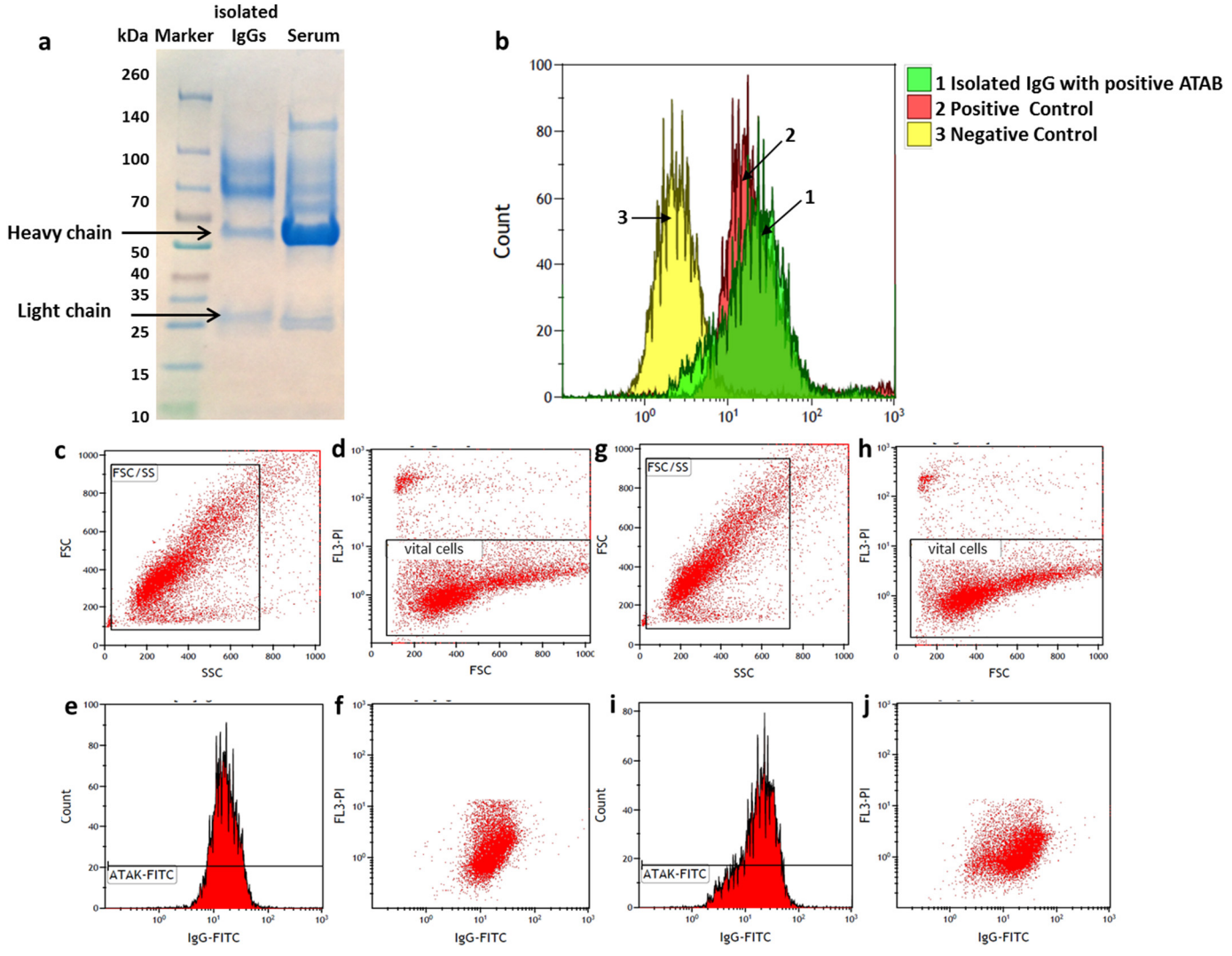

Fig. 2. Purified IgGs from ATAB-positive sera bind to JEG-3 cells. (a) SDS-PAGE analysis of purified IgGs from the sera of ATAB-positive patients and the corresponding sera of the same cases in a 4–15% gel after the Coomassie blue staining. Lanes (from left to right): pre-stained marker, purified IgGs, sera apart from purified IgGs. Arrows indicate the positions of heavy chain and light chain of purified IgGs, respectively. SDS-PAGE was repeated three times. (b) A representative flow cytometric diagram suggests ATAB-positive IgGs keep the ability of targeting JEG-3 cells as the ATAB-positive sera. Three merged peaks show (1) purified IgGs with positive ATAB, (2) positive control and (3) negative control. Flow cytometry data of positive control (c–f) and purified IgGs with positive ATAB (g–j). Forward scatter (FCS)/side scatter (SSC) plot of all the JEG-3 cells (c.g); FCS/PI plot (d.h); IgG-FITC plot (e.i); IgG-FITC/FL3-PI (f.j). Events were represented as red points.

5 μg/ml ATAB-negative IgGs (222·14 ± 25·08 mIU/ml, P = 0·128, Wilcoxon test, Fig. 3a) or by 10 μg/ml ATAB-negative IgGs (210·43 ± 18·33 mIU/ml, P = 0·091, Wilcoxon test, Fig. 3b) in comparison to the control (228·1 ± 20·04 mIU/ml) after 12 h of incubation. Unfortunately, progesterone was not detected in the supernatants of JEG-3 cells.

Incubation with 50 μg/ml ATAB-positive IgGs for 24 h promoted PAI-1 expression level by 11·9% compared with the control group (0·51 ± 0·05 μg/ml vs 0·46 ± 0·05 μg/ml, P = 0·027, Wilcoxon test, Fig. 3c), whereas 5 μg/ml and 10 μg/ml had no effects on PAI-1 production in JEG-3 cells (0·50 ± 0·08 μg/ml, 0·49 ± 0·07 μg/ml vs 0·46 ± 0·05 μg/ml, Wilcoxon test, Fig. 3c). Extending the incubation time to 36 h, 5, 10 and 50 μg/ml ATAB-positive IgGs induced PAI-1 levels in cell culture supernatants by 30·8%, 18·6% and 40·1% with P values 0·028, 0·027 and 0·043, respectively (Wilcoxon test, Fig. 3d). In contrast, ATAB-negative IgGs did not alter the production of PAI-1 in JEG-3 cells independently of incubation time and IgGs concentration (Fig. 3e.f).

3.3. Targets of ATAB

In order to identify possible antigens targeted by ATAB, we first applied 1-dimensional (1D) western blot (WB) combined with mass spectrometry (MS). 1D WB showed an obvious single band with the molecular weight between 35 and 40 kDa (Fig. 4a). The MS analysis of the corresponding band of a Coomassie stained gel identified 330 proteins out of 322 protein families (Supplementary Table 5). The mass spectrometry data have been deposited to the PRIDE repository with the dataset identifier PXD012478 [19]. To further increase the protein separation, we performed 2D WB. The excision of corresponding spots in a Coomassie stained 2D gel and subsequent MS analysis revealed a reactivity of ATAB against poly(rC)-binding protein 1 (PCBP1) and heterogeneous nuclear ribonucleoprotein D-like (HNRPDL) and α-Enolase (ENO1), which were also identified in the 1D gel within the molecular weight range of the WB signal.

ENO1 has been known as a target of autoimmune antibodies in a variety of autoimmune diseases [20–22]. Therefore we hypothesized that ENO1 could represent a target of ATAB (Supplementary Fig. 2).

To test this, we analyzed if the production of β-hCG and progesterone in JEG-3 cells is influenced by a commercially available anti-ENO1 antibodies. The level of β-hCG was decreased by 16·35% after 36 h incubation with 1 ng/ml anti-ENO1 antibodies compared to the control antibody (5·46 ± 0·87 vs 6·27 ± 0·31 mIU/ml, P = 0·012, Wilcoxon test, Fig. 4b). 100 ng/ml and 1 μg/ml of anti-ENO1 antibodies suppressed the production of β-hCG by 16·93% (5·42 ± 0·43 mIU/ml, P = 0·012, Wilcoxon test) and 24·55% (4·93 ± 0·49 mIU/ml, P = 0·012, Wilcoxon test, Fig. 4b), respectively. However, the addition of 10 ng/ml of anti-ENO1 antibodies (P = 0·123, Wilcoxon test) or no addition (P = 0·799, Wilcoxon test, Fig. 4b) did not alter β-hCG expression in JEG-3 cells. The expression of progesterone was only decreased after 24 h incubation with 1 μg/ml anti-ENO1 antibodies compared with the control (1·57 ± 0·09 vs 1·718 ± 0·07 ng/ml, P = 0·012, Wilcoxon test, Fig. 4c). After incubation with 1, 10, 100 ng/ml anti-ENO1 antibodies,

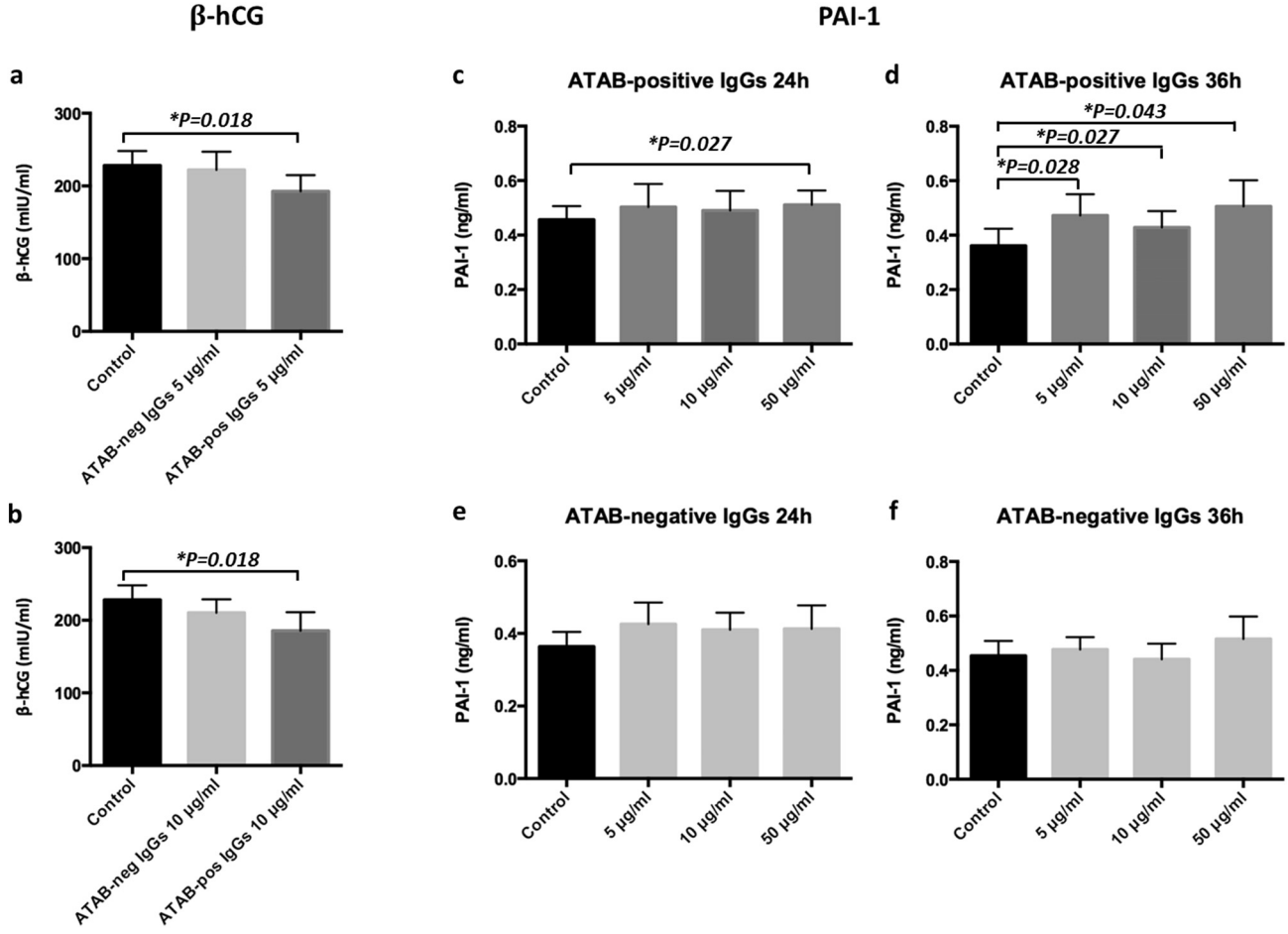

Fig. 3. Expression of β-hCG and PAI-1 is influenced by purified IgGs in JEG-3 cells. (a.b) The secretion of β-hCG in JEG-3 cells was inhibited by 5 μg/ml (a) and 10 μg/ml (b) of ATAB-positive IgGs compared with controls after incubating 12 h (P < 0·05, Wilcoxon test, n = 6), whereas ATAB-negative IgGs showed no effect. (c.d) The production of plasminogen activator inhibitor type 1 (PAI-1) in JEG-3 cells was increased by 50 μg/ml of ATAB-positive IgGs after 24 h of incubation and was enhanced by 5, 10 and 50 μg/ml after 36 h of incubation compared to the control (P < 0·05, Wilcoxon test, n = 6). (e.f) In contrast, ATAB-negative IgGs showed no effect on PAI-1 expression. Data were shown as mean ± SEM and P-values are shown individual treatment groups compared to control.

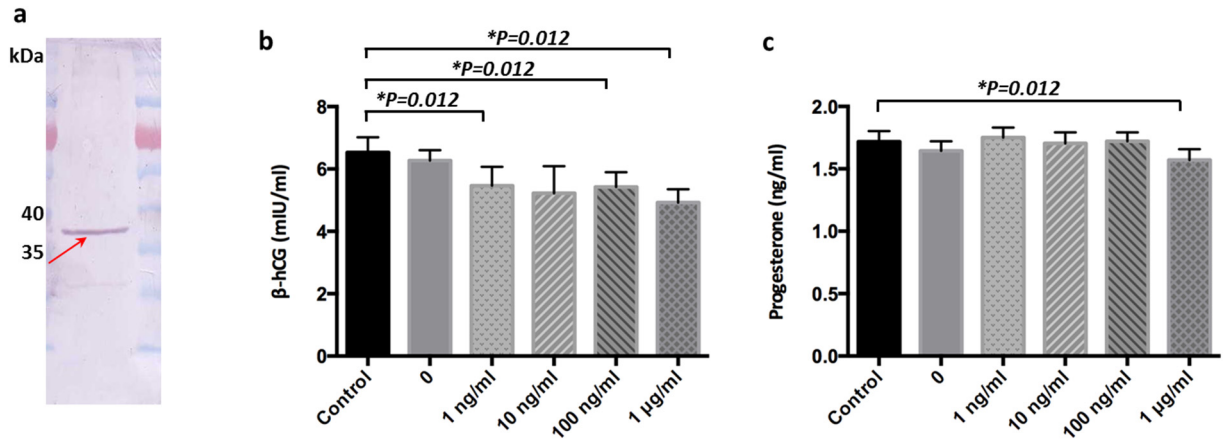

Fig. 4. Anti-ENO1 antibodies inhibit the expression of β-hCG and progesterone in JEG-3 cells. (a) An obvious band signal marked by an arrow was detected by 1 dimension western blot. JEG-3 proteins were used as antigens, 10 μg/ml ATAB-positive IgGs as the primary antibody and goat-anti-human antibodies as the secondary antibody. ENO1 was identified to be one of the most prominent targets with western blot and mass spectrometry. 1D western blots were repeated at least 5 times. (b.c) The production of β-hCG in JEG-3 cells was inhibited by 1, 100 and 1000 ng/ml of anti-ENO1 antibodies while the secretion of progesterone was suppressed by 1 μg/ml of anti-ENO1 antibodies compared to the rabbit polyclonal IgGs by ELISA ($P < 0{\cdot}05$, Wilcoxon test, $n = 6$). Data were shown as mean ± SEM and P-values are shown individual treatment groups compared to isotype control.

progesterone levels in JEG-3 cells remained unaffected (each $P > 0{\cdot}1$, Wilcoxon test, Fig. 4c).

3.4. Confirmation of anti-ENO1 antibody binding

In order to further determine that ATAB antibodies can bind to ENO1, we carried out competitive assays. Importantly, incubation of anti-ENO1 antibodies (10 μg/ml) and ATAB-positive IgGs (10 μg/ml) decreased the signals in western blots of JEG-3 membrane (Fig. 5a). Further, binding of ATAB-positive IgGs to JEG-3 cells was reduced by approximately 50% ($15{\cdot}66 \pm 2{\cdot}42$ vs $31{\cdot}61 \pm 3{\cdot}46$, $P = 0{\cdot}043$, Wilcoxon test, Fig. 5b.c, Supplementary Fig. 3) when 0·4 mg/ml anti-ENO1 antibodies and 2 mg/ml ATAB-positive IgGs were mixed. Pre-incubating 2 mg/ml ATAB-positive IgGs with 20 μg recombinant ENO1 proteins at 4 °C for 1 h also attenuated the binding between JEG-3 cells and ATAB-positive IgGs compared with the group without pre-incubation ($19{\cdot}16 \pm 2{\cdot}84$ vs $31{\cdot}61 \pm 3{\cdot}46$, $P = 0{\cdot}043$, Wilcoxon test, Fig. 5d.e, Supplementary Fig. 3) or with pre-incubation with 20 μg BSA ($24{\cdot}3 \pm 2{\cdot}06$ vs $31{\cdot}61 \pm 3{\cdot}46$, $P = 0{\cdot}043$, Wilcoxon test, Fig. 5d.e). Since anti-ENO1 antibodies can compete with ATAB-positive IgGs and bind to JEG-3 cells, we conclude that ENO1 is a prominent target of ATABs in JEG-3 cells.

3.5. Effect of anti-ENO1 antibodies on HVT cells

To further confirm that ENO1 is a prominent target of ATABs, we applied primary human villous trophoblast (HVT) cells as an in vitro trophoblast model. Anti-ENO1 antibodies decreased the production of β-hCG in HVT cells in a concentration dependent manner. 1, 10, and 100 ng/ml of anti-ENO1 antibodies decreased β-hCG production by 10·30% ($7{\cdot}39 \pm 0{\cdot}31$ mIU/ml, $P = 0{\cdot}008$, Mann-Whitney test, Fig. 6a), 20·05% ($6{\cdot}59 \pm 0{\cdot}44$ mIU/ml, $P = 0{\cdot}018$, Mann-Whitney test, Fig. 6a) and 28·56% ($5{\cdot}89 \pm 0{\cdot}49$ mIU/ml, $P = 0{\cdot}028$, Mann-Whitney test, Fig. 6a) in HVT cells compared with the isotype control ($8{\cdot}24 \pm 0{\cdot}29$ mIU/ml), respectively. Progesterone secretion in the isotype group ($7{\cdot}93 \pm 0{\cdot}15$ ng/ml) was suppressed to $7{\cdot}22 \pm 0{\cdot}21$ ng/ml ($P = 0{\cdot}008$, Mann-Whitney test, Fig. 6b), $7{\cdot}36 \pm 0{\cdot}18$ ng/ml ($P = 0{\cdot}028$, Mann-Whitney test, Fig. 6b) and $7{\cdot}14 \pm 0{\cdot}27$ ng/ml ($P = 0{\cdot}012$, Mann-Whitney test, Fig. 6b) by 1, 10, and 100 ng/ml of anti-ENO1 antibodies, respectively.

3.6. Anti-ENO1 antibodies are increased in sera of ATAB-positive patients

ENO1 autoimmune antibodies have been intensively investigated in the context of rheumatoid arthritis together with others, including autoantibodies against γ-Enolase, citrullinated fibrinogen (CFG) and modified citrullinated vimentin (MCV) [21]. Therefore, the levels of these four autoimmune antibodies in the sera of uRM patients were determined by ELISA and compared between the ATAB-positive group and ATAB-negative group. Neither maternal age, gravidity nor parity differed between the ATAB-positive ($n = 30$) and the ATAB-negative ($n = 36$, each P values>.05, student's *t*-test) groups (Supplementary Table 2). The level of anti-α-Enolase antibodies was nearly doubled in serum of ATAB-positive patients compared to ATAB-negative patients ($7{\cdot}04 \pm 1{\cdot}80$ vs $3{\cdot}68 \pm 0{\cdot}54$ ng/ml, $P = 0{\cdot}007$, student's *t*-test, Fig. 7a). Additionally, the level of anti-MCV antibodies were 33·2% higher in the sera of positive ATAB patients than in negative ATAB patients ($44{\cdot}75 \pm 4{\cdot}67$ vs $35{\cdot}21 \pm 1{\cdot}73$ U/ml, $P = 0{\cdot}018$, student's *t*-test, Fig. 7d). However, no correlation was found between levels of anti-ENO1 and anti-MCV antibodies in uRM patients ($P = 0{\cdot}216$, Pearson correlation $= 0{\cdot}198$). Furthermore, neither the level of anti-γ-Enolase antibodies differed significantly between the ATAB-positive group and ATAB-negative group ($3{\cdot}92 \pm 0{\cdot}43$ vs $4{\cdot}20 \pm 0{\cdot}40$ ng/ml, $P = 0{\cdot}890$, student's *t*-test, Fig. 7b), nor the level of anti-CFG antibodies ($60{\cdot}76 \pm 12{\cdot}10$ vs $64{\cdot}01 \pm 11{\cdot}20$ ng/ml, $P = 0{\cdot}907$, student's *t*-test, Fig. 7c).

3.7. ENO1 is more abundant in the decidua of uRM patients

Since anti-ENO1 antibodies were more abundant in serum of ATAB-positive patients, we also investigated the expression of ENO1 in the first trimester placenta of 20 uRM patients and 22 healthy controls by immunohistochemistry. Mean age, mean gestational age and parity times were similar between uRM patients and healthy controls, while the gravidity times was lower in uRM patients ($3{\cdot}11 \pm 1{\cdot}08$) compared to healthy subjects ($3{\cdot}42 \pm 1{\cdot}90$, $P = 0{\cdot}002$, student's *t*-test, Supplementary Table 1). In the syncytium, significant difference of ENO1 expression was not observed between uRM patients and healthy controls (IRS $6{\cdot}36 \pm 2{\cdot}01$ vs $6{\cdot}80 \pm 1{\cdot}88$, $P = 0{\cdot}467$, Mann-Whitney test, Fig. 8a–c). In the decidua, the IRS score of ENO1 staining in uRM patients is $5{\cdot}26 \pm 2{\cdot}49$, significantly higher than in healthy controls (IRS $= 3{\cdot}67 \pm 1{\cdot}72$, $P = 0{\cdot}038$, Mann-Whitney test, Fig. 8d–f). The positive and negative controls are showed in Supplementary Fig. 4.

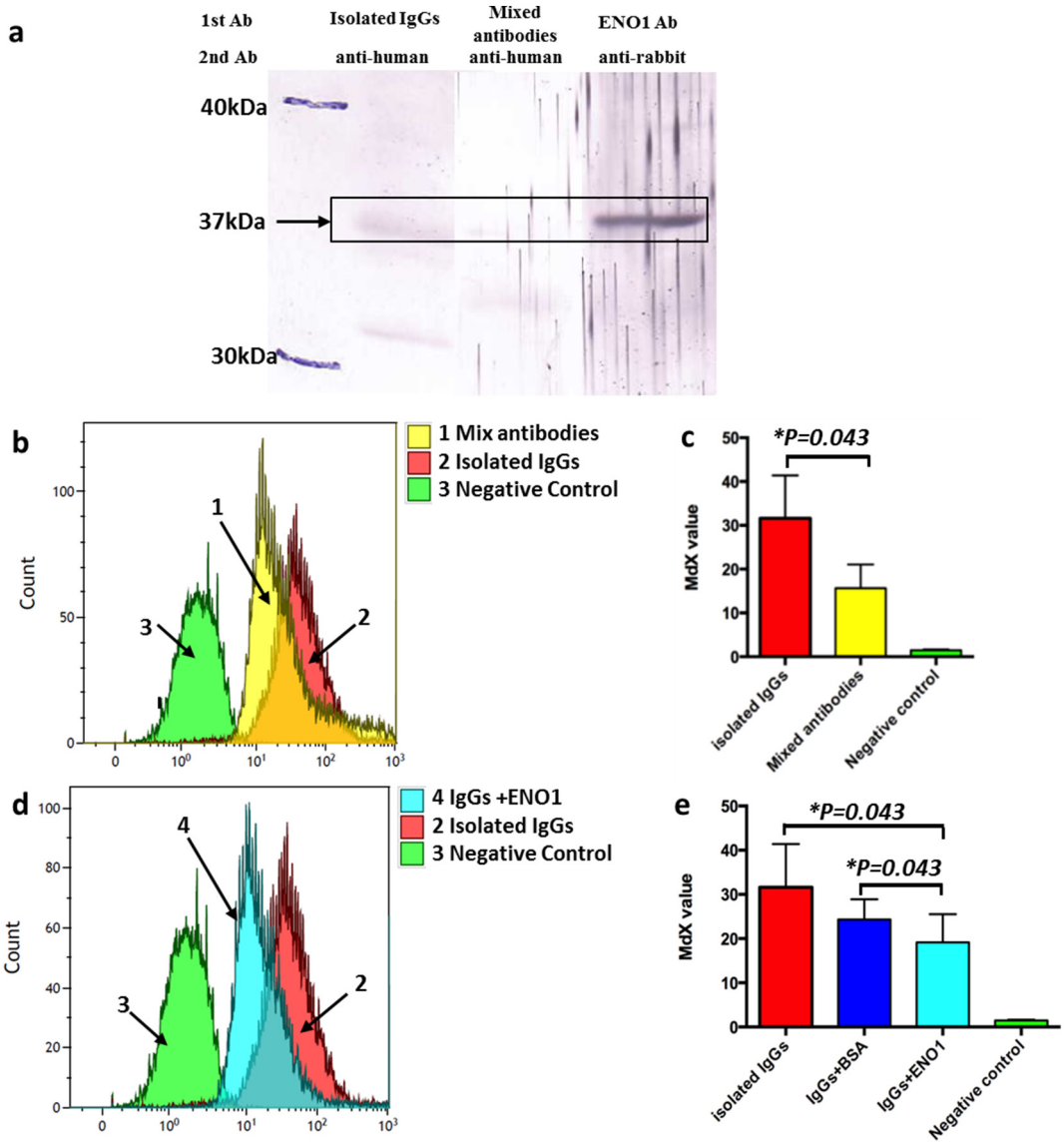

Fig. 5. Anti-ENO1 antibodies are a member of ATAB. (a) The signals of ENO1 in JEG-3 cells were reduced by incubation with a mixture of antibodies (10 μg/ml rabbit anti-ENO1 antibodies and 10 μg/ml human ATAB-positive IgGs) compared with only 10 μg/ml incubating human purified IgGs or 10 μg/ml rabbit anti-ENO1 antibodies. Different secondary antibodies were used in western blots: goat-anti-human antibody, goat-anti-human antibody and goat-anti-rabbit antibody (from left to right rows). (b.c) The diagram shows that in the flow cytometry mixed antibodies (0·42 mg/ml anti-ENO1 antibodies with 2 mg/ml isolated IgGs) bind less JEG-3 cells as ATAB-positive IgGs ($P < 0·05$, Wilcoxon test, $n = 3$). (d.e) Pre-incubating 20 μg recombinant human ENO1 protein with 2 mg/ml ATAB-positive IgGs decreases the binding of ATAB-positive IgGs to JEG-3 cells ($P < 0·05$, Wilcoxon test, $n = 3$). The MCS values are showed with mean ± SD and P-values are shown individual treatment groups compared to incubation with ATAB-positive IgGs.

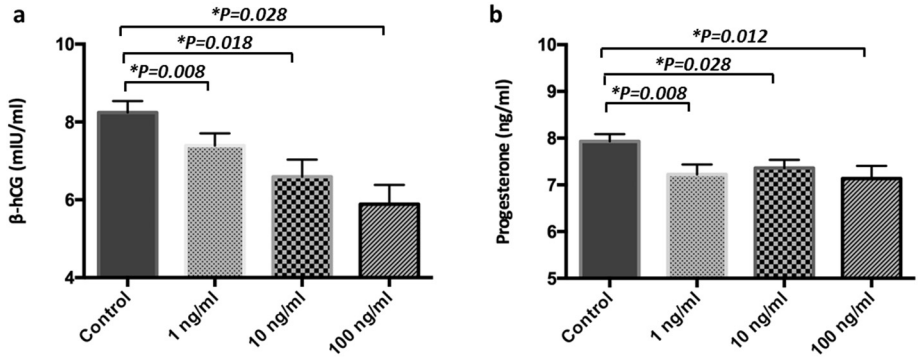

Fig. 6. Anti-ENO1 antibodies inhibit the expression of β-hCG and progesterone in human villous trophoblast (HVT) cells. (a) The production of β-hCG in HVT cells was inhibited by 1, 10 and 100 ng/ml of anti-ENO1 antibodies in a dose dependent manner. (each P value <0·05, Wilcoxon test, $n = 6$). (b) The secretion of progesterone in HVT cells was suppressed by 1, 10 and 100 ng/ml of anti-ENO1 antibodies in a dose dependant manner. (each P value <0·05, Wilcoxon test, $n = 6$). Values are expressed as shown as mean ± SEM and P-values are shown individual treatment groups compared to isotype control.

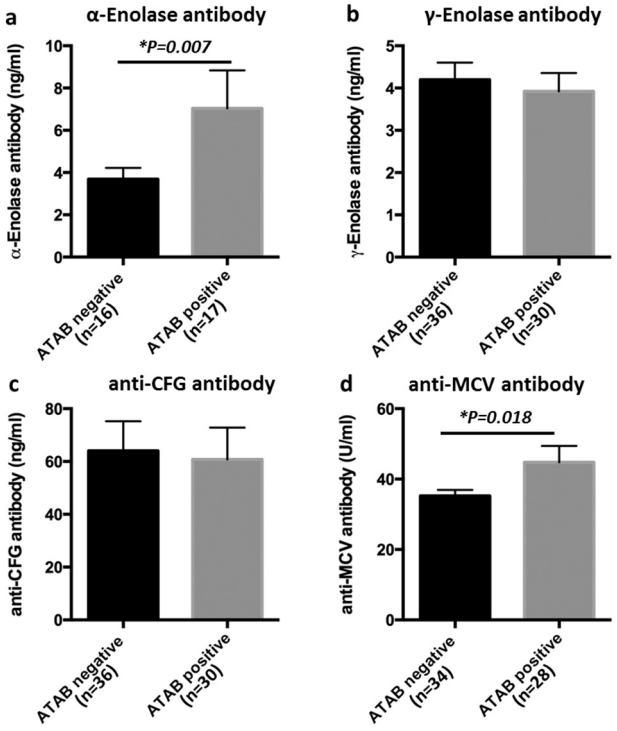

Fig. 7. Anti-ENO1 titers are higher in the sera of ATAB-positive patients. (a) Anti-ENO1 antibodies were increased in the 16 uRM patients with positive ATAB compared with 17 cases with negative ATAB ($P = 0{\cdot}007$, student's *t*-test). (b,c) The levels of anti-γ-Enolase antibodies and anti-citrullinated fibrinogen (CFG) antibodies were not changed in 36 ATAB-positive patients and 30 ATAB-negative cases (both $P > 0{\cdot}05$, student's *t*-test). (d) Anti-MCV antibodies were higher in the sera of 34 ATAB-positive patients than 28 ATAB-negative cases ($P = 0{\cdot}018$, student's *t*-test). Data were shown as mean ± SEM and statistically significant differences between two uRM groups were marked with P values.

Triple immunofluorescence staining was applied to localize ENO1 expressing cells in the first trimester placenta and HLA-G was used as a maker for extravillous trophoblasts (EVT). ENO-1 was present in the cytoplasm of EVT in the first trimester placenta. Both ENO1 and β-arrestin 2 were co-expressed with HLA-G predominantly in the cytoplasm of EVT, especially in the uRM group (Fig. 9).

4. Discussion

ATAB are more prevalent in serum of uRM patients compared to healthy controls [12], and the definition of ATAB is restricted to JEG-3 cells in our previous study [12]. Based on this, uRM patients were divided in ATAB-positive and ATAB-negative uRM patients. Sera from ATAB-positive women can inhibit the production of β-hCG and progesterone in trophoblast JEG-3 cells [14]. In the current study, we observed that purified IgGs of ATAB-positive patients maintained the capacity to target JEG-3 cells, thereby decreasing β-hCG secretion and increasing PAI-1 production. Furthermore, we identified ENO1 as a target of ATAB by western blots and mass spectrometry. ENO1 is a multifunctional glycolytic enzyme expressed abundantly in the cytosol and its molecular weight is approximately 45 kDa. The main role of ENO1 is to catalyse the conversion of 2-phosphoglycerate to phosphoenolpyruvate in glycolysis [23]. We detected ENO1 in the choriocarcinoma cell line JEG-3 as well as in the EVT of the first trimester placenta.

ENO1 can induce autoantibodies in many cancers [24] and autoimmune diseases [20] via overexpression, mutation, misfolding, aberrantly degradation or location [25,26]. Until now, there is no conclusive explanation for why α-Enolase becomes an autoantigen. Translocation of ENO1 to the cell surface can drive the production of specific ENO1 autoantibodies, causing autoimmune diseases. In the infarcted heart, β-arrestin associates with ENO1 and translocates together to the cell membrane as auto-antigens, thus inducing high levels of anti-ENO1 and anti-arrestin antibodies in patients' sera [27]. We confirmed the co-expression of ENO1 and β-arrestin in EVT in the first trimester placenta of uRM patients (Fig. 9). β-arrestin plays a role in G-protein

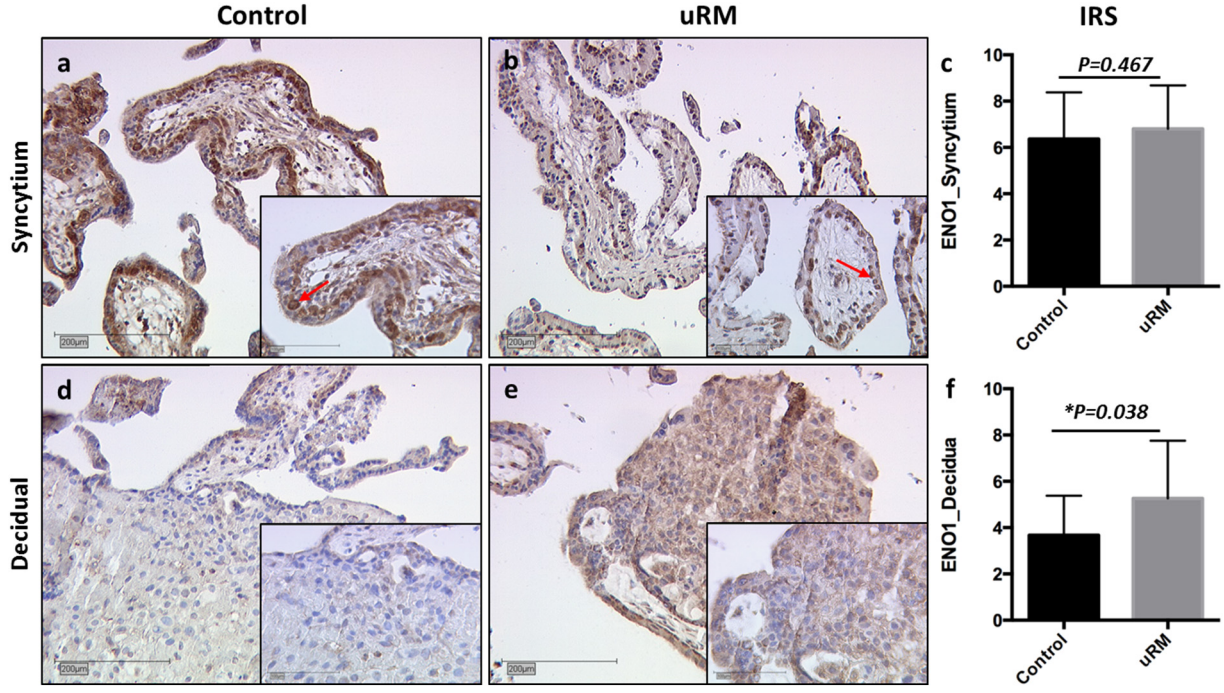

Fig. 8. ENO1 expression is increased in the decidua of uRM patients in the first trimester. Immunohistological analyses of ENO1 expression in the first trimester placenta were measured among 20 uRM patients and 22 healthy controls by IRS scores. (a–c) In the syncytium, the staining of ENO1 did not show significant difference in uRM patients (a) and controls (b), which is represented as bar charts ($P > 0{\cdot}05$, Mann-Whitney test). The strong staining of ENO1 in the syncytium is marked with red arrows. (d–f) In the decidua, the expression of ENO1 was higher in uRM patients (d) as in controls (e, $P = 0{\cdot}038$, Mann-Whitney test). Magnification × 10 lens, scale bar = 200 μm; magnifications of inserted pictures are ×25 lens, scale bar = 100 μm. uRM = unexplained recurrent miscarriages.

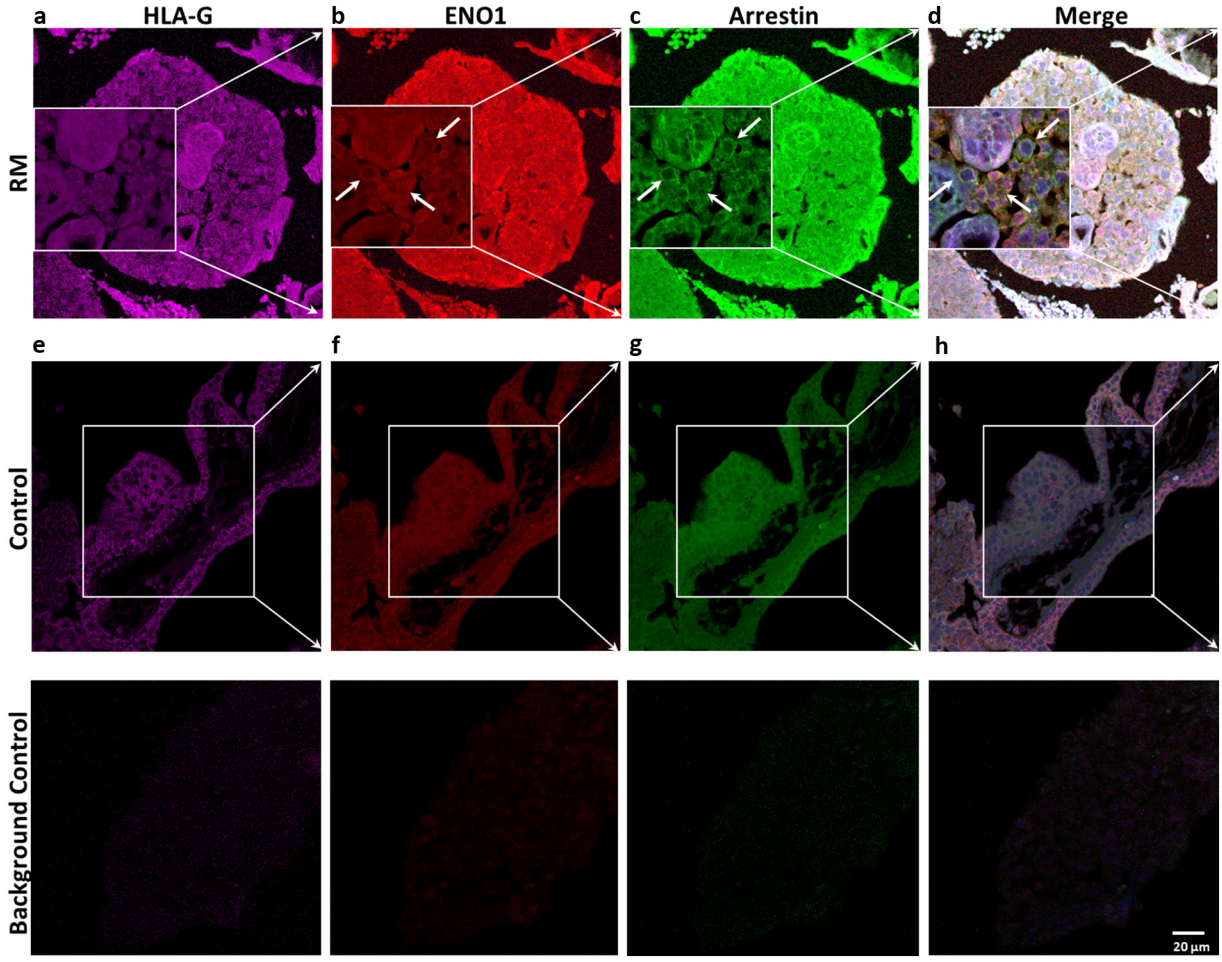

Fig. 9. ENO1 coexpresses with β-arrestin in the extravillous trophoblasts (EVT) of uRM patients and healthy controls. Confocal microscopy images showed a co-localization of ENO1 (red) and β-arrestin (green) in EVT of the first trimester placenta in uRM women (a–d) and healthy controls (e–h), which are shown with white arrows. HLA-G is used as the marker for EVT (magenta), magnification x20, scale bar =20 μM.

receptor desensitization, receptor endocytosis, activation of extracellular signal regulated kinases and other mitogen activated protein kinases [27]. ENO1 can also be translocated to the cell surface by extracellular peptidyl arginine deiminase [20] and lipopolysaccharides [28].

Overexpression of ENO1 may induce the production of anti-ENO1 antibodies. This notion is supported by increased expression of ENO1 in the decidua of the first trimester placenta of uRM patients. Under the situation of shallow trophoblast invasion and impaired placental hypoxia, overexpression of genes encoding for glycolytic enzymes is an adoptive response, and may lead to ENO1 overexpression [29]. Increased ENO1 levels were also found in proliferating microglia and astrocytes after spinal cord injury in adult rats [30], implying that ENO1 is associated with ischemia and hypoxia. Breast cancer MCF-7 cells adapt to hypoxia by increasing ENO1 mRNA and decreasing MBP-1 translation [31], which additionally hints that ENO1 is a more relevant target of ATAB than MBP-1. Gharesi-Fard et al. observed that ENO1 expression is decreased in the placenta of uRM patients compared with normal late first trimester placentas in the protein level [32]. However, this study involved only 5 placenta tissues in each group, which were from 14 to 15 gestational weeks of the first trimester. We used placenta tissues of 20 uRM patients and 22 healthy controls in the early first trimester (approximately 9 gestational weeks). Additionally, compared to normal tissue, ENO1 is subjected to elevated acetylation, methylation and phosphorylation in carcinomas [24]. Anti-ENO1 antibodies are directed against two upregulated ENO1 isoforms that are phosphorylated in Ser 419 among pancreatic cancer patients [33,34]. The posttranslational modifications of ENO1 in uRM patients were not addressed in our study and could be explored in future studies.

Autoantibodies against ENO1 are associated with a variety of autoimmune and inflammatory diseases, such as systemic lupus erythematosus, rheumatoid arthritis, systematic sclerosis, Behçet's disease, ulcerative colitis, Crohn's disease, primary sclerosing cholangitis and retinopathy [20], endometriosis, premature ovarian failure and asthma [22]. ENO1 was found to be a specific antigen for anti-endometrial antibodies in sera of endometriosis patients [35]. Sarapik et al. suggested that anti-ENO1 IgA antibodies are more prevalent in tubal factor infertility patients instead of endometriosis patients, and contribute to lower pregnancy rates [22]. The level of anti-ENO1 antibodies in the sera was enhanced in ATAB-positive uRM patients than ATAB-negative cases. This indicates that anti-ENO1 autoimmune antibodies may influence reproductive performance.

Increased ENO1 can contribute to high levels of cyclic adenosine monophosphate (cAMP) in the preterm heart [36], which stimulates the transcription of hCG gene in villous trophoblasts by interacting with the cAMP response element-binding protein (CREB) [37]. It suggests anti-ENO1 antibodies might decrease the expression of hCG via downregulation of cAMP and CREB in JEG-3 cells, and low expression of hCG can contribute to miscarriages. ENO1 also functions as a plasminogen receptor on cell membranes and exhibits an important role in modulating the fibrinolytic system [38]. Anti-ENO1 antibodies suppress tumor metastasis via urokinase-type plasminogen activator, urokinase-type plasminogen activator receptor, and plasminogen [39]. The

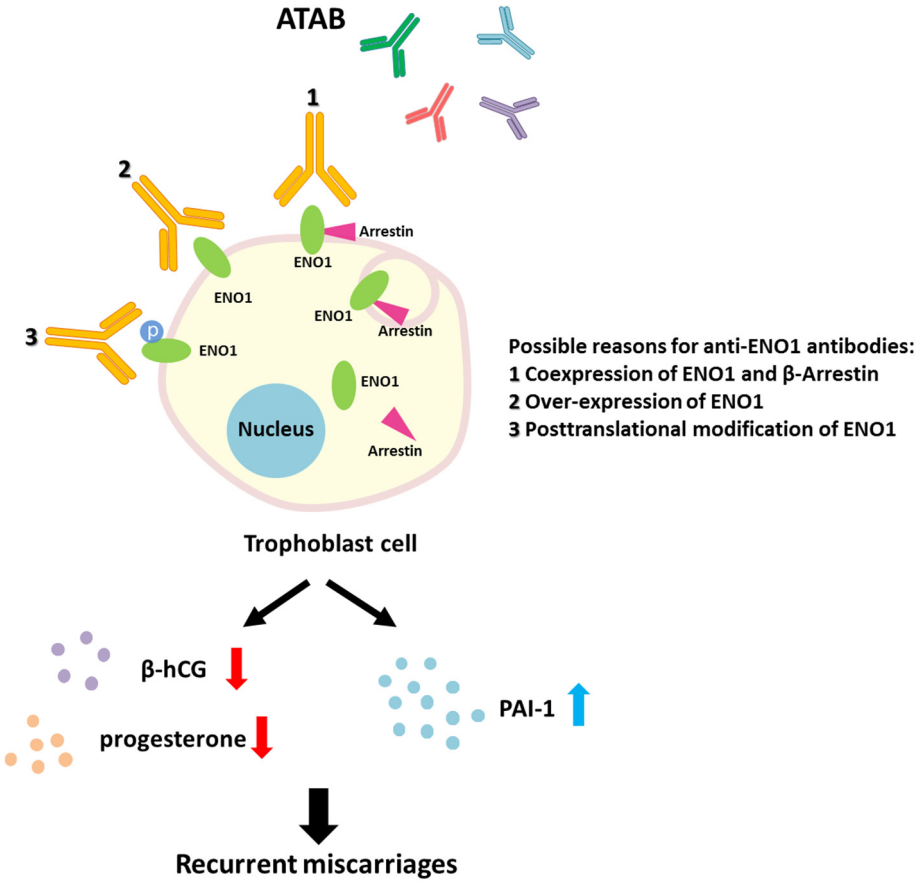

Fig. 10. The possible role of ENO1 in unexplained recurrent miscarriages (uRM). Anti-ENO1 antibodies are among the antitrophoblast antibodies (ATAB) and are higher expressed in the sera of positive-ATAB uRM patients. The translocation (1), overexpression (2) or posttranslational modifications (3) of ENO1 in the extravillous trophoblasts may be the reason for induction of anti-ENO1 antibody expression in the sera of uRM patients. Anti-ENO1 antibodies can inhibit the production of β-hCG and progesterone in trophoblast cells, and may stimulate the expression of PAI-1. All these changes may eventually contribute to recurrent miscarriages.

purified IgGs with positive-ATAB can enhance PAI-1 production in JEG-3 cells. High plasma levels of PAI-1 and high PAI activities are present in uRM women in comparison to healthy controls [40]. The increased expression of PAI-1 can prevent extracellular matrix degradation, causing shallow trophoblast invasion and eventually miscarriages [41]. This indicates that anti-ENO1 antibodies may inhibit EVT cells migration and invasion by upregulating PAI-1 expression and downregulating hCG production in uRM. The impacts of other cytokines on the invading trophoblast in RM are mostly unknown [42]. The positive feedback between ENO1 and pro-inflammatory cytokines (IL-1β, TNF-α and PGE_2) creates a pro-inflammatory environment [20], which also exerts adverse effects on pregnancy maintenance.

We here confirmed that ATAB contain anti-ENO1 autoantibodies targeting trophoblast cells. However, it remains unclear if further trophoblast antigens are target by ATAB influencing implantation and pregnancy outcome. O'Dwyer et al. demonstrated that both ENO1 and γγ-enolase are autoimmune targets shared by the pituitary and placenta in patients with lymphocytic hypophysitis [43]. γγ-enolase is localized in syncytiotrophoblast, decidua and the vascular smooth muscle of anchoring and terminal villi [43]. However, amounts of anti-γγ-enolase antibodies did not differ between the ATAB-positive and ATAB-negative patients. In contrast, anti-MCV autoantibody levels were increased in ATAB-positive women in comparison to ATAB-negative women, suggesting anti-MCV antibodies may also contribute to ATAB. A limitation of our research is that we did not examine all the autoimmune diseases among uRM patients, especially for rheumatoid arthritis and lymphocytic hypophysitis. Additionally, the placenta samples were not matched to the sera samples of uRM patients. Our group has recently observed that the ATAB reactivity can be downregulated by pre-incubating uRM patients' sera with 10 mg/ml IVIG [15]. The mRNA and protein abundance of ENO1 can be reduced by liver X receptor agonist GW3965 or T0901317 in J774-A1 murine macrophage cell line [44]. ENO1 has a shorter protein variant MBP-1 with a molecular weight of 37 kDa [45]. MBP-1 is localized in the nucleus and acts as a transcriptional repressor of c-myc proto-oncogene, which subsequently regulates cell growth and differentiation [45,46]. These additional antigens of ATAB, such as MBP-1, will be investigated in future studies.

In summary, we observed the abundance of ENO1 in the first trimester placenta of uRM patients. Consequently, anti-ENO1 antibodies levels were increased in ATAB-positive patients. Generation of anti-ENO1 antibodies is likely associated with the translocation and overexpression of ENO1 on the cell surface of EVT. In vitro, anti-ENO1 antibodies inhibit the production of β-hCG and progesterone in JEG-3 and HVT cells, which could potentially contribute to miscarriages. Therefore, anti-ENO1 antibodies may represent an autoimmune biomarker for uRM. Further research is needed to determine the suitability of eliminating anti-ENO1 antibodies or decreasing ENO1 expression as a therapeutic strategy in ENO1-related autoimmune diseases (Fig. 10).

Supplementary data to this article can be found online at https://doi.org/10.1016/j.ebiom.2019.02.027.

Author contributions

U.J conceived and designed the study; C·K performed the immunohistochemistry, M.K conducted 2D western blots and mass spectrometry, H·I and C·S performed the triple fluorescence imaging; N.R and C.J.T initiated the flow cytometry assay and collected clinical data; T.F,

S.M and G.J.A analyzed and interpreted the data; Y·Y performed 1D western blotting, ELISA, and wrote the manuscript; T.F, U.J, CJT and V·S revised the manuscript. All other authors read and approved the manuscript.

Funding

Y·Y was recipient of a scholarship from the China Scholarship Council. H.I.A. and C.S. were supported by the SFB914, projects Z01 and A10, respectively. The sponsors did not participate in the study design, data analysis or the manuscript writing.

Declaration of interests

No author has conflict of interest to declare.

Acknowledgements

We thank Martina Rahmeh and Anna Krieger for technical assistance with regard to human villous trophoblast cells culture and hormone detection. Y.Y. received a grant from the China Scholarship Council. H.I.A. would like to thank the German Research Council (SFB914, Project Z01 & A10) for Support.

References

[1] Practice Committee of American Society for Reproductive M. Definitions of infertility and recurrent pregnancy loss: a committee opinion. Fertil Steril 2013;99(1):63.
[2] Ford HB, Schust DJ. Recurrent pregnancy loss: etiology, diagnosis, and therapy. Rev Obstet Gynecol 2009;2(2):76–83.
[3] Practice Committee of the American Society for Reproductive M. Evaluation and treatment of recurrent pregnancy loss: a committee opinion. Fertil Steril 2012;98(5):1103–11.
[4] Shahine L, Lathi R. Recurrent pregnancy loss: evaluation and treatment. Obstet Gynecol Clin N Am 2015;42(1):117–34.
[5] Choudhury SR, Knapp LA. Human reproductive failure I: immunological factors. Hum Reprod Update 2001;7(2):113–34.
[6] Gregori S, Amodio G, Quattrone F, Panina-Bordignon P. HLA-G orchestrates the early interaction of human trophoblasts with the maternal niche. Front Immunol 2015;6:128.
[7] Michita RT, Zambra FMB, Fraga LR, Sanseverino MTV, Callegari-Jacques SM, Vianna P, et al. A tug-of-war between tolerance and rejection - new evidence for 3'UTR HLA-G haplotypes influence in recurrent pregnancy loss. Hum Immunol 2016;77(10):892–7.
[8] Meuleman T, Haasnoot GW, van Lith JMM, Verduijn W, Bloemenkamp KWM, Claas FHJ. Paternal HLA-C is a risk factor in unexplained recurrent miscarriage. Am J Reprod Immunol 2018;79(2).
[9] Coulam CB, Acacio B. Does immunotherapy for treatment of reproductive failure enhance live births? Am J Reprod Immunol 2012;67(4):296–304.
[10] Kajino T, McIntyre JA, Faulk WP, Cai DS, Billington WD. Antibodies to trophoblast in normal pregnant and secondary aborting women. J Reprod Immunol 1988;14(3):267–82.
[11] Motak-Pochrzest H, Malinowski A. The occurrence of immunological disturbances in patients with recurrent miscarriage (RM) of unknown etiology. Neuro Endocrinol Lett 2013;34(7):701–7.
[12] Rogenhofer N, Ochsenkuhn R, von Schonfeldt V, Assef RB, Thaler CJ. Antitrophoblast antibodies are associated with recurrent miscarriages. Fertil Steril 2012;97(2):361–6.
[13] Burt D, Johnston D, Rinke de Wit T, Van den Elsen P, Stern PL. Cellular immune recognition of HLA-G-expressing choriocarcinoma cell line Jeg-3. Int J Cancer Suppl 1991;6:117–22.
[14] von Schonfeldt V, Rogenhofer N, Ruf K, Thaler CJ, Jeschke U. Sera of patients with recurrent miscarriages containing anti-trophoblast antibodies (ATAB) reduce hCG and progesterone production in trophoblast cells in vitro. J Reprod Immunol 2016;117:52–6.
[15] Rogenhofer N, von Schonfeldt V, Ochsenkuhn R, Sili F, Thaler CJ. Effects of polyvalent immunoglobulins in patients with recurrent pregnancy loss and antibodies to the choriocarcinoma cell line JEG-3. Eur J Obstet Gynecol Reprod Biol 2015;194:161–7.
[16] Ye Y, Vattai A, Ditsch N, Kuhn C, Rahmeh M, Mahner S, et al. Prostaglandin E2 receptor 3 signaling is induced in placentas with unexplained recurrent pregnancy losses. Endocr Connect 2018;7(5):749–61.
[17] Jeschke U, Karsten U, Reimer T, Richter DU, Bergemann C, Briese V, et al. Stimulation of hCG protein and mRNA in first trimester villous cytotrophoblast cells in vitro by glycodelin a. J Perinat Med 2005;33(3):212–8.
[18] Remmele W, Stegner HE. Recommendation for uniform definition of an immunoreactive score (IRS) for immunohistochemical estrogen receptor detection (ER-ICA) in breast cancer tissue. Pathologe 1987;8(3):138–40.
[19] Vizcaino JA, Csordas A, del-Toro N, Dianes JA, Griss J, Lavidas I, et al. 2016 update of the PRIDE database and its related tools. Nucleic Acids Res 2016;44(D1):D447–56.
[20] Bae S, Kim H, Lee N, Won C, Kim HR, Hwang YI, et al. Alpha-enolase expressed on the surfaces of monocytes and macrophages induces robust synovial inflammation in rheumatoid arthritis. J Immunol 2012;189(1):365–72.
[21] Kastbom A, Forslind K, Ernestam S, Geborek P, Karlsson JA, Petersson IF, et al. Changes in the anticitrullinated peptide antibody response in relation to therapeutic outcome in early rheumatoid arthritis: results from the SWEFOT trial. Ann Rheum Dis 2016;75(2):356–61.
[22] Sarapik A, Haller-Kikkatalo K, Utt M, Teesalu K, Salumets A, Uibo R. Serum anti-endometrial antibodies in infertile women - potential risk factor for implantation failure. Am J Reprod Immunol 2010;63(5):349–57.
[23] Chen SH, Giblett ER. Enolase: human tissue distribution and evidence for three different loci. Ann Hum Genet 1976;39(3):277–80.
[24] Capello M, Ferri-Borgogno S, Cappello P, Novelli F. Alpha-enolase: a promising therapeutic and diagnostic tumor target. FEBS J 2011;278(7):1064–74.
[25] Shih NY, Lai HL, Chang GC, Lin HC, Wu YC, Liu JM, et al. Anti-alpha-enolase autoantibodies are down-regulated in advanced cancer patients. Jpn J Clin Oncol 2010;40(7):663–9.
[26] Tan HT, Low J, Lim SG, Chung MC. Serum autoantibodies as biomarkers for early cancer detection. FEBS J 2009;276(23):6880–904.
[27] Mirshahi M, Le Marchand S. Co-purification of arrestin like proteins with alpha-enolase from bovine myocardial tissues and the possible role in heart diseases as an autoantigen. Biochem Biophys Res Commun 2015;460(3):657–62.
[28] Wygrecka M, Marsh LM, Morty RE, Henneke I, Guenther A, Lohmeyer J, et al. Enolase-1 promotes plasminogen-mediated recruitment of monocytes to the acutely inflamed lung. Blood 2009;113(22):5588–98.
[29] Pringle KG, Kind KL, Sferruzzi-Perri AN, Thompson JG, Roberts CT. Beyond oxygen: complex regulation and activity of hypoxia inducible factors in pregnancy. Hum Reprod Update 2010;16(4):415–31.
[30] Li M, Wen H, Yan Z, Ding T, Long L, Qin H, et al. Temporal-spatial expression of ENOLASE after acute spinal cord injury in adult rats. Neurosci Res 2014;79:76–82.
[31] Sedoris KC, Thomas SD, Miller DM. Hypoxia induces differential translation of enolase/MBP-1. BMC Cancer 2010;10:157.
[32] Gharesi-Fard B, Zolghadri J, Kamali-Sarvestani E. Alteration in the expression of proteins in unexplained recurrent pregnancy loss compared with in the normal placenta. J Reprod Dev 2014;60(4):261–7.
[33] Zhou W, Capello M, Fredolini C, Piemonti L, Liotta LA, Novelli F, et al. Mass spectrometry analysis of the post-translational modifications of alpha-enolase from pancreatic ductal adenocarcinoma cells. J Proteome Res 2010;9(6):2929–36.
[34] Tomaino B, Cappello P, Capello M, Fredolini C, Sperduti I, Migliorini P, et al. Circulating autoantibodies to phosphorylated alpha-enolase are a hallmark of pancreatic cancer. J Proteome Res 2011;10(1):105–12.
[35] Walter M, Berg H, Leidenberger FA, Schweppe KW, Northemann W. Autoreactive epitopes within the human alpha-enolase and their recognition by sera from patients with endometriosis. J Autoimmun 1995;8(6):931–45.
[36] Tsuzuki Y, Takeba Y, Kumai T, Matsumoto N, Mizuno M, Murano K, et al. Antenatal glucocorticoid therapy increase cardiac alpha-enolase levels in fetus and neonate rats. Life Sci 2009;85(17–18):609–16.
[37] Knofler M, Saleh L, Strohmer H, Husslein P, Wolschek MF. Cyclic AMP- and differentiation-dependent regulation of the proximal alphaHCG gene promoter in term villous trophoblasts. Mol Hum Reprod 1999;5(6):573–80.
[38] Plow EF, Das R. Enolase-1 as a plasminogen receptor. Blood 2009;113(22):5371–2.
[39] Hsiao KC, Shih NY, Fang HL, Huang TS, Kuo CC, Chu PY, et al. Surface alpha-enolase promotes extracellular matrix degradation and tumor metastasis and represents a new therapeutic target. PLoS One 2013;8(7):e69354.
[40] Gris JC, Neveu S, Mares P, Biron C, Hedon B, Schved JF. Plasma fibrinolytic activators and their inhibitors in women suffering from early recurrent abortion of unknown etiology. J Lab Clin Med 1993;122(5):606–15.
[41] Ye Y, Vattai A, Zhang X, Zhu J, Thaler CJ, Mahner S, et al. Role of plasminogen activator inhibitor type 1 in pathologies of female reproductive diseases. Int J Mol Sci 2017;18(8).
[42] Makhseed M, Raghupathy R, Azizieh F, Farhat R, Hassan N, Bandar A. Circulating cytokines and CD30 in normal human pregnancy and recurrent spontaneous abortions. Hum Reprod 2000;15(9):2011–7.
[43] O'Dwyer DT, Clifton V, Hall A, Smith R, Robinson PJ, Crock PA. Pituitary autoantibodies in lymphocytic hypophysitis target both gamma- and alpha-enolase - a link with pregnancy? Arch Physiol Biochem 2002;110(1–2):94–8.
[44] De Boussac H, Maqdasy S, Trousson A, Zelcer N, Volle DH, Lobaccaro JM, et al. Enolase is regulated by liver X receptors. Steroids 2015;99(Pt B):266–71.
[45] Subramanian A, Miller DM. Structural analysis of alpha-enolase. Mapping the functional domains involved in down-regulation of the c-myc protooncogene. J Biol Chem 2000;275(8):5958–65.
[46] Maranto C, Perconti G, Contino F, Rubino P, Feo S, Giallongo A. Cellular stress induces cap-independent alpha-enolase/MBP-1 translation. FEBS Lett 2015;589(16):2110–6.